TISSUE ENGINEERING: Part A
Volume 21, Numbers 11 and 12, 2015

DOI: 10.1089/ten.tea.2014.0317

Original Article

Mechanical Characterization and Shape Optimization of Fascicle-Like 3D Skeletal Muscle Tissues Contracted with Electrical and Optical Stimuli

Devin Neal, PhD,[1] Mahmut Selman Sakar, PhD,[2] Rashid Bashir, PhD,[3] Vincent Chan, PhD,[1] and Haruhiko Harry Asada[1]

In this study, we present a quantitative approach to construct effective 3D muscle tissues through shape optimization and load impedance matching with electrical and optical stimulation. We have constructed long, thin, fascicle-like skeletal muscle tissue and optimized its form factor through mechanical characterization. A new apparatus was designed and built, which allowed us to measure force–displacement characteristics with diverse load stiffnesses. We have found that (1) there is an optimal form factor that maximizes the muscle stress, (2) the energy transmitted to the load can be maximized with matched load stiffness, and (3) optical stimulation using channelrhodopsin2 in the muscle tissue can generate a twitch force as large as its electrical counterpart for well-developed muscle tissue. Using our tissue construct method, we found that an optimal initial diameter of 500 μm outperformed tissues using 250 μm by more than 60% and tissues using 760 μm by 105%. Using optimal load stiffness, our tissues have generated 12 pJ of energy per twitch at a peak generated stress of 1.28 kPa. Additionally, the difference in optically stimulated twitch performance versus electrically stimulated is a function of how well the overall tissue performs, with average or better performing strips having less than 10% difference. The unique mechanical characterization method used is generalizable to diverse load conditions and will be used to match load impedance to muscle tissue impedance for a wide variety of applications.

Introduction

Formation of an engineered skeletal muscle tissue *in vitro* can have a range of engineering and medical applications. Successful construction of such a muscle tissue can not only shed light on the muscle formation process[1] but can also open the door to creating organ mimics for drug screening and drug development, replacing expensive animal models, especially if the essential mechanics and biology can be recapitulated in the *in vitro* system. Similarly, developing *in vitro* methodologies for muscle formation will allow engineers to build medical implants using biological materials,[2] realize novel soft robotics and biological machines, and interface these synthetic components with other naturally occurring systems.

To accomplish these goals, muscle constructs must act on a load, producing mechanical work and transmitting it to the load. Understanding of basic force–displacement characteristics and output power transmission is a prerequisite for designing and building those machines and implants. Yet, quantitative and detailed mechanical work performance of *in vitro* skeletal muscles has been reported only in a few articles, but with a limited scope. This is primarily because of the complexity of muscle mechanics. The force generated by a muscle construct varies significantly depending on numerous conditions, including displacement, prestress, velocity, and load impedance, as well as fatigue, creep, and stress relaxation.[3–5] In the past, rather simple methods have been used for evaluating mechanical performance.

A common practice to characterize the muscle tissue is to measure the isometric tension generated. This is the measurement of the force generated while the tissue maintains a constant length by holding the two ends of the tissue at a constant position relative to each other throughout the measurement. The length may be maintained either by coupling it to rigid supports or by applying feedback position control of the ends. Feedback position control has been used as far back as 1965 when muscle from a live frog was tested to determine the relationship between sarcomere length and isometric tension generation.[5] *In vitro*-grown 3D muscle tissue constructs have been tested using stiff couplings.[6]

[1]Department of Mechanical Engineering, Massachusetts Institute of Technology, Cambridge, Massachusetts.
[2]Institute of Robotics and Intelligent Systems, ETH Zurich, Zurich, Switzerland.
[3]Electrical and Computer Engineering, University of Illinois at Urbana-Champaign, Urbana, Illinois.

Isometric force measurements cannot provide information on the energy that can be imparted on a load for a single muscle twitch. Isometric force measurements are useful in finding peak forces achievable by muscle tissue and in comparing muscle tissue formed under various conditions, such as testing effects of various influences like alignment, drugs, or damage. However, isometric force measurements cannot provide information on all time and displacement-dependent parameters describing the muscle contraction such as power or twitch energy. Twitch energy transmissibility is critically important for cardiac tissue as well as for any engineered mechanical system powered by muscle tissue (biobots).[7]

With the addition of velocity control, a typical isometric muscle testing apparatus may be used to measure power output directly by testing isovelocity shortening.[4] However, this power measured is dependent on the magnitude of the velocity, and a constant velocity is not necessarily the condition in which the muscle will be functioning.

An alternative method of characterizing skeletal muscle tissue performance is to have the muscle tissue work against a load such as a known linear stiffness. With this aim, muscle tissue structures have been grown such that their two terminal ends are supported by the ends of two compliant posts.[8–10] This method allows for the direct measurement of muscle tissue output energy transmitted to a load. However, the performance of any given tissue can only be assessed for driving a single load, that is, the stiffness of the cantilevered posts. Fully characterizing the tissues against various loads is not possible with this method. Thus, the performance of the tissue under loads it may face in physiological or engineered settings cannot be assessed directly from these prior reported structures. Additionally, it is impossible to remove the muscle tissue from the posts' devices without damaging or altering its performance in the process. One final concern with using polymer posts is that their stiffness is influenced by many factors. The Young's modulus of PDMS can change by roughly a factor of two simply by changing curing temperature,[11] and other factors such as temperature and deformation rate also change its compliance.[12] Polymers are viscoelastic; therefore, the resting stiffness must be measured separately from the short-term activation stiffness of polymer posts.

In this study, we present a systematic method and apparatus for evaluating the mechanical performance of *in vitro*-grown muscle constructs without using isometric contractions or a single linear elastic load. The presented method allows for the testing of tissue performance against any load, and a single tissue sample may be tested against any number of loads. This method allows us to (1) measure force–displacement characteristics, (2) tune the prestrain applied to the muscle construct, (3) vary the stiffness of load impedance, and (4) quantify the work produced by the muscle construct. Using this quantitative mechanical performance evaluation method, we address how 3D skeletal muscle constructs can be optimized with respect to (1) form factor and morphology and (2) matching with the load stiffness. The primary objective of morphology evaluation here is to determine the optimal diameter at which to grow 3D aligned muscle tissue having a high density of contractile proteins. We find that optimal load impedance exists for a particular muscle construct to transmit the mechanical work. Specifically, performance is assessed in terms of maximum work transmitted to a load due to a single stimulated twitch cycle. Force and/or displacement may also be used in twitch performance comparison because these two values are monotonically coupled to the work performed.

The method of inducing contractions of muscle cells is another important factor when characterizing tissue. Three methods of stimulation have been used for engineered tissue characterization: chemical,[13] electrical,[14] and optical.[9] Chemical and electrical stimulation involve potentially invasive changes to the cellular environment and do not offer the same potential for tight spatial and temporal resolution as optical stimulation. Optical stimulation is a newer technique, in which cells are transfected with DNA encoding the optogenetic protein channelrhodopsin-2 (ChR2). Characterization of optical stimulation with comparison with an alternative form of stimulation has not been reported. The benefits of high spatial and temporal control of optogenetics over other forms of stimulation have already been used for high-throughput testing *in vitro*[9] and will eventually provide utility in clinical applications when combined with developing optical technologies.[15]

The method presented here facilitates both electrical and optical stimulation for coherent comparison. It also facilitates the quantification of mechanical performance by elongating the tissue through lateral displacement. Lateral displacement entails displacing a tissue construct at a point between its two anchored ends in a direction perpendicular to the primary axis of the tissue. Lateral displacement for mechanical characterization has been used for neurite characterization[16] as well as for very simple skeletal muscle characterization.[13] Muscle tissue made through the sacrificial outer mold method described previously[17] facilitates this mechanical characterization method in two ways. First, the tissue is anchored between the stiff well walls of the culture device, ensuring no serial compliance at the anchor points that would affect measurements. This is in contrast to tissue developed on compliant posts. Second, the tissue can be tested without transferring the tissue to another substrate or measurement device. This is in contrast to the methods of producing muscle constructs, which require at least one anchor to be decoupled from the culture dish on which the tissue is grown.[6] Multiple cantilever probes of different stiffness may be used on a single tissue. This allows for the testing of tissue against different mechanical loads. Isometric and post-based methods alone are incapable of testing a single tissue against differing loads. By changing the load, it is possible to determine the load impedance that matches the specific tissue to maximize the output work of the tissue. However, this method has never been used to characterize muscle tissue grown under varying conditions, nor with different cantilever probe stiffnesses and displacements.

Materials and Methods

Muscle strip tissue constructs

Fascicle-like muscle tissue constructs were produced as described previously.[17] For the experiments presented here, the sacrificial mold material consisted of 5% w/v porcine gelatin (Sigma-Aldrich), 10 U/mL thrombin (Sigma-Aldrich), and 1% 0.5 N NaCl in phosphate-buffered saline (Lonza),

and the cell solution consisted of 5 mg/mL fibrinogen (Sigma-Aldrich), 10^7 cells/mL, and 0.5 mg/mL aminocaproic acid (Sigma-Aldrich). The cells used were C2C12 cells (ATCC) transfected with ChR2 as described previously.[9] Growth media consist of 10% fetal bovine serum (Sigma-Aldrich) in Dulbecco's modified Eagle's medium (DMEM; ATCC) and 0.5 mg/mL aminocaproic acid. Differentiation media contain 10% horse serum (Sigma-Aldrich), DMEM (ATCC), and 0.5 mg/mL aminocaproic acid.

Briefly, sacrificial mold material was injected at 37°C into 5-mm-diameter PDMS (Dow Corning) wells containing a steel pin (McMaster Carr) spanning the well. The mold material was then cooled to room temperature to solidify. Removal of the pins leaves a 5 mm long cylindrical cavity in the gelatin in the 5-mm-diameter well.

This cavity is then filled with a cell/hydrogel solution. The device is then immediately placed in a 37°C incubator where the gelatin mold melts releasing thrombin and where the hydrogel solution solidifies. The sacrificial mold solution is then gradually diluted with daily media changing. Growth media are used for the first 2 days. Differentiation media are used after the first 2 days. Fascicle-like muscle constructs produced using this method are shown in Figure 1a.

For the experiments in which the pin diameter was the independent variable, two separate experiments were run. The first consisted of three devices with two strips in each device using each of the following nominal pin diameters: 0.010″ (254 μm), 0.012″ (305 μm), 0.014″ (356 μm), and 0.020″ (508 μm). The second consisted of three devices using each of the following nominal pin diameters: 0.014″ (356 μm) and 0.020″ (508 μm), 0.030″ (762 μm), and 0.040″ (1016 μm).

For the optical versus electrical stimulation experiment and the variable probe stiffness experiments, three devices of two strips each were used and nominal pin diameters used were 0.020″ (508 μm).

For all experiments, stimulated contraction testing was performed 14 days after cell seeding.

Force and displacement measurement using a lateral cantilever probe

The basic concept of the force probe is to laterally displace the tissue strip at its center using the end of a cantilever probe of known stiffness. As diagramed in Figure 1b and c, the center of the tissue displaces in the direction orthogonal to the undisplaced tissue axis. As the tip of the cantilever displaces the center of the strip, the length of the strip elongates and the cantilever bends. Measuring the position of the cantilever base and tip, and knowing the stiffness of the cantilever, we can find the force of the probe, F_{probe}, exerted on the tissue:

$$F_{probe} = k_{probe}(x_{base} - x_{tip}) \quad (1)$$

where x_{tip} is the lateral displacement of the cantilever tip, x_{base} is the lateral displacement of the cantilever base, and k_{probe} is the stiffness of the cantilever probe as shown in Figure 1.

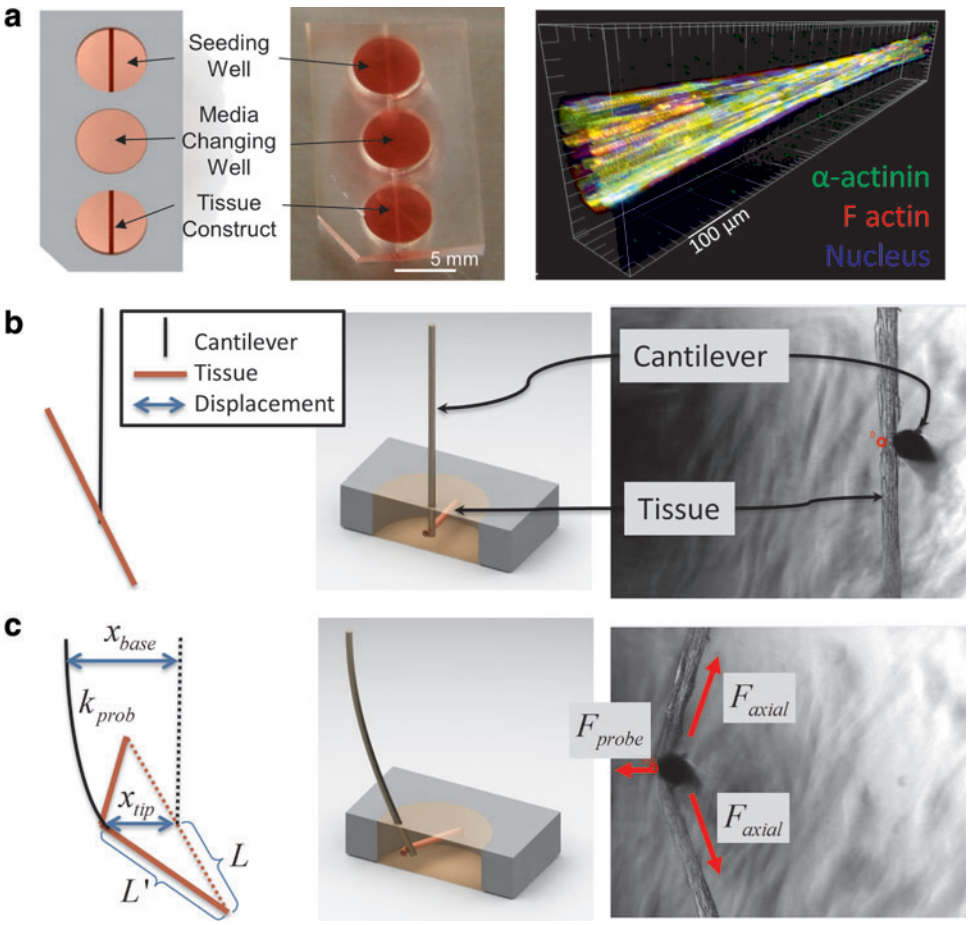

FIG. 1. Muscle strip tissue construct and force probe diagram. **(a)** Schematic and image of tissue culture device along with confocal image of the muscle strip consisting of numerous muscle cells in a device. **(b)** Diagram, solid model, and image of cantilever in contact with tissue with no displacement. **(c)** Diagram, solid model, and image of cantilever tip displacing tissue due to displacement of cantilever base. x_{tip} is the lateral displacement of the cantilever tip, x_{base} is the lateral displacement of the cantilever base, and k_{probe} is the cantilever stiffness. L and L' are the unforced and forced half-lengths of the tissue, respectively. F_{probe} is the force on the probe tip, and F_{axial} is the force along the axis of the tissue. Color images available online at www.liebertpub.com/tea

The geometric relationships relevant to displacement through cantilever probes are shown in Supplementary Figure S1 (Supplementary Data are available online at www.liebertpub.com/tea). Combining geometric relations, force balance, and Hooke's law, we derive expressions for the axial force along the tissue, F_{axial}, and the displaced length of half the tissue, L'. From the diagram, we obtain the following:

$$\frac{F_{axial,x}}{F_{axial}} = \frac{x_{tip}}{L'} \tag{2}$$

$$x_{tip} = \sqrt{L'^2 - L^2} \tag{3}$$

where $F_{axial,x}$ is the lateral component of the axial force held by the tissue, and L and L' are the unforced and forced half-lengths of the tissue, respectively.

A simple force balance along the direction of displacement is as follows:

$$F_{probe} = 2F_{axial,x} \tag{4}$$

Combining these equations yields an expression for the elongated length, L', and axial force, F_{axial}, of the tissue:

$$L' = \sqrt{x_{tip}^2 + L^2} \tag{5}$$

$$F_{axial} = (x_{base} - x_{tip})\frac{k_{probe}}{2x_{tip}}\sqrt{x_{tip}^2 + L^2} \tag{6}$$

From these equations, we can determine both axial force of the tissue and tissue elongation.

Characterization system

For this concept to work, (1) we must be able to finely adjust the position of the base of the cantilever, x_{base}, (2) the positions of the cantilever base, x_{base}, and tip, x_{tip}, must be measured simultaneously, and (3) the muscle tissue must be excitable. A new custom-built system that achieves these requirements is presented in Figure 2. The base of the cantilever is positioned with a three-axis stage assembly coupled to the cantilever probe through a stiff custom-machined aluminum beam. For the three-axis stage assembly, the x position (probe displacement direction) is controlled using both a manual stage (Thorlabs MT1/M) and a motorized stage (Thorlabs MT1/M-Z8), and y and z positions are controlled with a two-axis manual stage (Thorlabs DT12XZ/M). The three-axis stage assembly is rigidly mounted to the microscope stage. The probe cantilevers and electrodes are superglued to easily interchangeable 3D-printed couplings that easily snap onto the end of the aluminum beam in a repeatable manner. This quick snap method allows for numerous cantilever probes of any desired stiffness to be quickly interchanged while collecting data. The position of the base of the cantilever is measured with a laser micrometer (Micro-Epsilon optoNCDT 1401), which measures the position of a 3D-printed laser micrometer flag attached to the aluminum beam that extends away from the sample. The position of the tip is measured through images from a microscope. Video recorded on the microscope computer and the time history data from the laser micrometer are combined to give time-dependent data. To excite the muscle tissue electrically, electrodes that are attached to the cantilever base extend into the sample well and terminate with ends that are parallel to the strip.

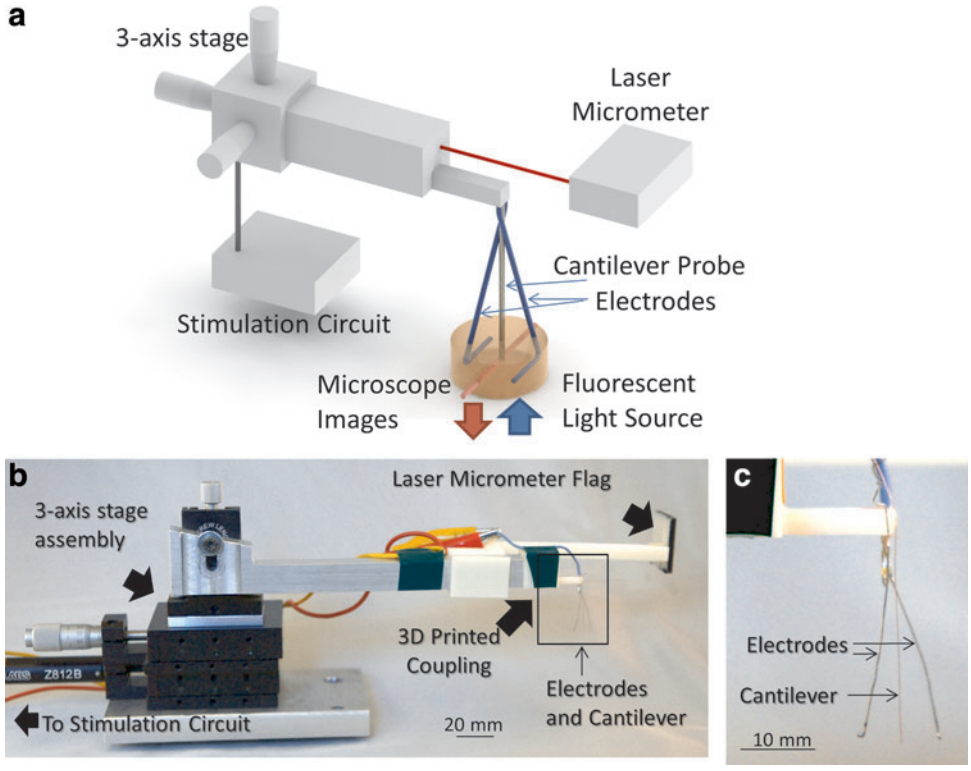

FIG. 2. Mechanical characterization system. **(a)** Schematic of mechanical characterization system. **(b)** Key components of mechanical characterization system. **(c)** A 3D-printed tip with a cantilever probe and electrodes. Color images available online at www.liebertpub.com/tea

Cantilever stiffnesses were evaluated before and after testing to ensure that the stiffnesses were consistent and that they were not plastically deformed during testing. The stiffnesses were evaluated by hanging known weights from the tip against gravity.

For all experiments, multiple twitches were generated through stimulation at the same prestrain conditions. In this system, prestrain was created by laterally displacing the cantilever probe to the point where $\sim 2\%$ strain was generated along the direction of the tissue strip. The base of the probe is fixed, and then contraction stimuli are applied.

This system is a general force transducer and may be adapted to other applications demanding measurements of small forces and small displacements, such as characterization of microposts,[9] or other biological materials. The only adaptation necessary for these and other applications would be to produce 3D-printed couplings with probes specific to the application.

To provide electrical stimulation to the muscle strips, electrodes were built into the system that would be capable of providing an electric field across the strip. Platinum electrodes are parallel to the strip to generate a uniform field across its length. The electrodes are at the precise depth of the tissue and independent of the displacement of the tissue as shown in Supplementary Figure S2a. The depths of the electrodes and probe tip are mechanically coupled to ensure that the depths of the electrodes and the probe tip are the same. To allow the probe tip and tissue to move independently of the electrodes upon displacement, compliant cantilevered electrodes rigidly coupled to the base of the cantilever tip were used. The electrodes are platinum wires coupled closely to the cantilever tip and splay out away from the cantilever probe as they extend down. When unforced, the two electrodes are separated by approximately three times the width of the sample well at their ends (Supplementary Fig. S2b). When inserted into the sample well, the electrodes must first be brought together with tweezers (Supplementary Fig. S2c). The elastic energy stored in the compliant electrodes keeps them pinned to the walls of the sample well even as the system translates the cantilever probe (Supplementary Fig. S3).

For electrical stimulation, an electric field of 30 V/cm was used with bipolar pulses of 1 ms each at a frequency of 1 Hz. The electric signal was controlled by an Arduino Uno microcontroller with custom scripts. For optical stimulation, a 300-W mercury lamp coupled with a GFP (473 nm wavelength) was used to generate 30 ms pulses at 1 Hz using custom scripts written into the microscope controlling software (Metamorph).

The magnitude of the stimulation, both optical and electrical, was selected to be high enough such that a 25% reduction in stimulation strength had no measurable change in stimulation-caused response. To address the concern of tissue penetration of the light stimulus, we made sure that the entire depth of tissue could be imaged using the stimulation strength of the light source. It is confirmed that because the tissue can be well imaged, stimulating light can penetrate the tissue.

Optical versus electrical stimulation response characterization

A single cantilever and pair of electrodes were used in the optical versus electrical stimulation experiments. The optical versus electrical stimulation protocol was designed to account for the effects of muscle fatigue. If we simply stimulated one way and then the other, muscle fatigue would make the second stimulation method appear worse due to fatigue of the strip. Six stimulation cycles were performed for each strip with 60 s of rest between each. Each stimulation cycle consisted of two subcycles with 60 s of rest between each. Each subcycle consisted of prestraining the tissue, stimulating the tissue five times with one form of stimuli (electric or optical), followed immediately by stimulating the tissue five times with the other form of stimuli (optical or electric), then relaxing the tissue. Using this protocol, muscle fatigue is factored out through averaging over all cycles. This protocol is shown in Supplementary Figure S4. The stiffness of the cantilever used was 0.0278 N/m.

Tissue response versus varying load characterization

Four different cantilevers with different stiffnesses were used in the variable stiffness experiment. Each strip was tested with each cantilever twice using the following protocol: the strip was displaced by the cantilever tip to a prestrained value of 2% strain and stimulated five times optically, then relaxed. For the diameter variation experiments, the protocol was the same as the variable stiffness experiment protocol, except only one cantilever probe was used. The stiffnesses used in the variable stiffness experiment were the following: 0.0038, 0.023, 0.11, and 0.65 N/m.

Tissue response as a function of diameter characterization

A single cantilever and pair of electrodes were used in the diameter variation experiments. Each strip was used to generate five twitches. The stiffness of the cantilever used was 0.0278 N/m.

Image and video analysis

Data from the laser micrometer (measuring cantilever probe base position) and the microscope camera video (measuring cantilever tip position) were processed to generate axial tissue force and displacement. The video data provide probe tip data with the use of open-source software called Tracker. Tracking the cantilever tip is robust and reliable, giving subpixel resolution. Each individual twitch was analyzed independently. This process is shown in Supplementary Figure S5. The tip and base data are synchronized based on a step-like input to the base position. Each twitch is segmented and combined with probe base data to determine axial strip displacement and force. Finally, each twitch is creep corrected assuming linear creep with a slope equal to the post-twitch position minus the pretwitch initial tip position divided by the twitch time. This creep correction is used to ensure that the data presented represent the force and displacements generated only by the contraction of the muscle.

Statistical analysis

In determining statistically significant differences, the means are compared using two-sampled *t*-tests.

Results

Optical versus electrical stimulation

Electric stimulation performance was slightly superior to optical stimulation performance overall. Figure 3 shows the wave forms and peak values of twitch forces induced by both optical and electrical stimuli. The peak force values of five twitches were evaluated for optical and electrical stimuli and for each of the six muscle strips having diverse levels of performance. The difference in the mean peak twitch force was less than 10% for stronger muscle strips. However, for poor performing strips, optical stimulation resulted in almost 40% worse mean twitch amplitude than electrical stimulation. Twitch data for the best performing strip, strip A (Fig. 3a), and the worst performing strip, strip C (Fig. 3b), exemplify this. The optically stimulated twitches nearly follow the electrically generated twitches for the high performing strip, strip A, while the optically generated twitches are generally much lower in force than the optically generated twitches for the poor performing strip, strip C. Aggregate data of the maximum twitch force generated for multiple strips with various overall performances (Fig. 3c) show that electric stimulation is mildly superior to optical stimulation. A trend can clearly be seen when the aggregate of the ratio of optical to electrical stimulation performance for each strip is plotted against mean maximum twitch force of the electrically stimulated twitches for each strip (Fig. 3d). This clearly demonstrates that as the overall performance of the strip increases, the relative performance of optically generated twitches approaches the performance of electrically generated twitches.

These results show that muscle constructs developed to a certain level may be stimulated optically and electrically with similar resulting contractions. This means that optical control of muscle tissue may be used for stimulation purposes in situations where electrodes are too intrusive or otherwise disadvantageous.

Maximum stress and optimal diameter

In Figure 4, multiple strips with diverse diameters are compared with respect to peak twitch force and stress. The largest twitch force was generated by the strip whose nominal pin diameter was 762 μm rather than 1016 μm (Fig. 4b). In terms of maximum peak stress, that is, peak force divided by the cross-sectional area, the 508 μm nominal diameter pin produced the maximum stress (Fig. 4a). The stress performance quickly drops off after this as the diameter increases. These results show that an optimal diameter exists for generating maximum stress. For the constructs formed using the smaller diameters (254, 305, and 356 μm), the mean stress generated is approximately the same and is independent of the initial diameter.

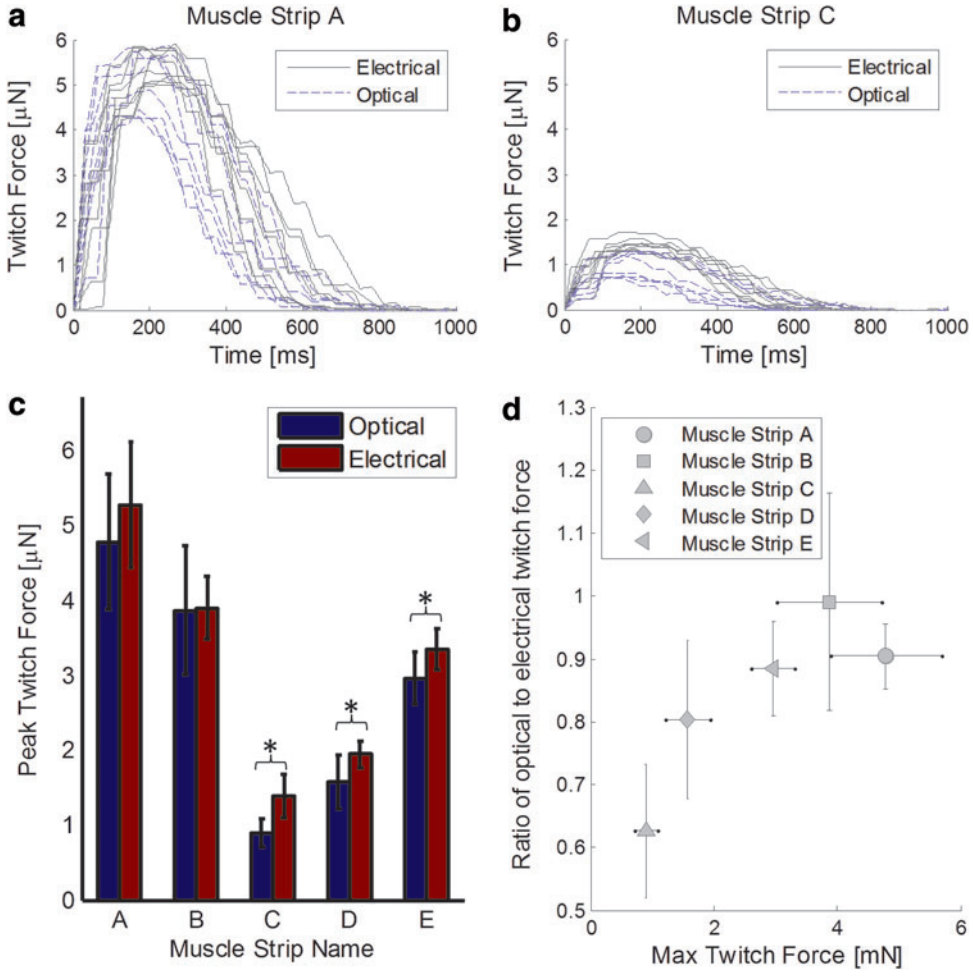

FIG. 3. Electric versus optical performance results. Exemplary twitch data for multiple optical and electrically stimulated twitches for a better than average performing strip **(a)** and less than average performing strip **(b)**. **(c)** Aggregate data of maximum twitch force achieved for numerous twitches stimulated through electrical and optical signals. **(d)** The ratio of optically to electrically stimulated maximum twitch force plotted against mean maximum twitch force generated electrically. *Asterisks* represent statistical differences with $p < 0.05$. Error bars are standard deviation values and n is 30 for each sample set. Color images available online at www.liebertpub.com/tea

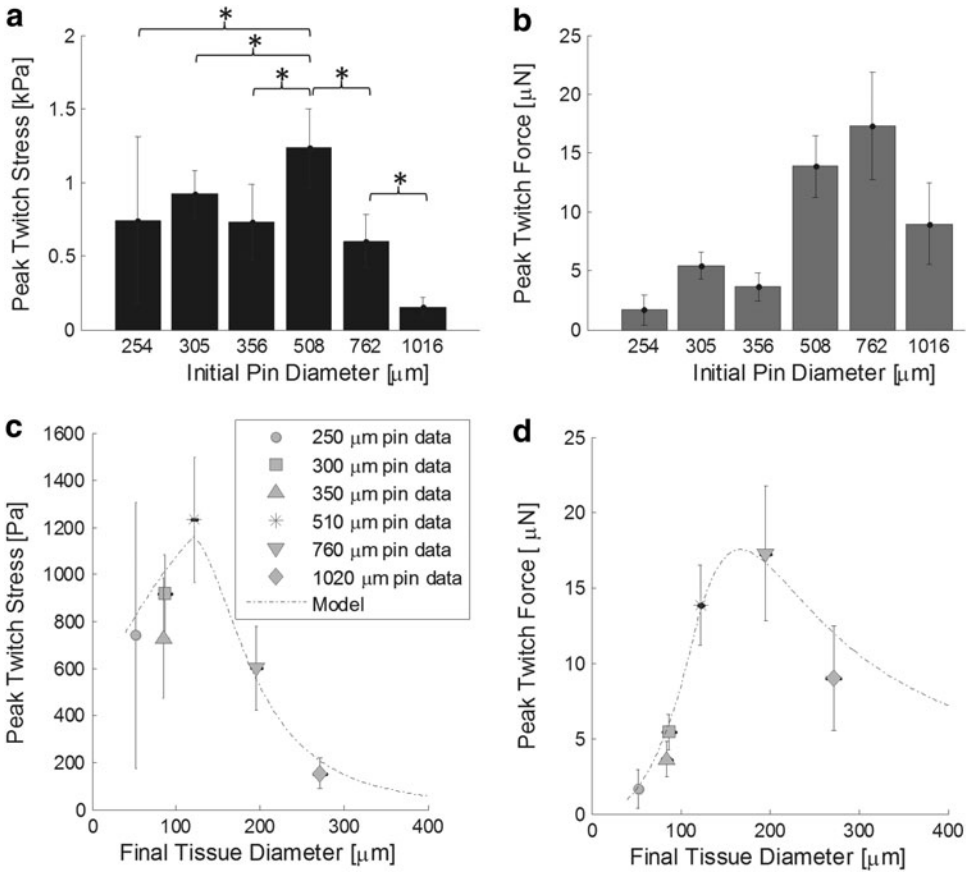

FIG. 4. Peak twitch stress and force over various initial pin diameters. Peak stress **(a)** and force **(b)** from twitches generated by constructs made using various initial nominal diameter pins. Initial pin diameter is a key controlled variable in maximizing final tissue stress output and is shown in **(a, b)** to emphasize the statistical significance of the peak stress magnitude achieved when using a pin diameter of 508 μm. *Asterisks* represent statistically significant differences with $p < 0.05$. Peak twitch stress **(c)** and force **(d)** plotted against a final construct diameter from constructs of differing initial pin diameters and a simple model that assumes (1) greater variability in tissue diameter along the length for smaller diameter tissues and (2) only the outer ~ 50 μm of the construct produces significant contractile stress due to diffusion-limited processes during development. Compaction of the tissue from the initial pin diameter to final tissue diameter is more dramatic for smaller diameter molds. All error bars are standard deviations and n is 30 for each sample set.

Note that the standard deviation in peak twitch stress is much greater for the smallest diameter pins used (Fig. 4a). There exists a greater degree of nonuniformity for the smaller diameter strips, as described previously.[17] Figure 5 shows the confocal images of the strips and their cross sections. The diameter of the strip varies along the longitudinal direction. The cross section at the end of the small-diameter strip (Fig. 5a) contains only one myotube (shown as a colored circle), while the center cross section has at least three myotubes. The local stiffness of the narrow region tends to be lower than that of thicker regions. Narrower regions of the construct act as compliant elements connected in series with the rest of the construct. These compliant weak links absorb displacement with the elastic tissue, decreasing the resulting output force (Fig. 4b). The larger diameter strips have more uniform cross sections throughout the strip, leading to the larger force generation (Fig. 5b).

Generated energy and load matching

The twitches of a single muscle construct working against multiple cantilever probes of diverse stiffnesses are shown in Figure 6. Each data point represents the combination of peak twitch displacement and force measured with a single probe. The stiffer the cantilever, the larger the peak twitch force and lower the peak twitch displacement (Fig. 6a). A linear fit matches the force–displacement curve with an r^2 value of 0.955. This shows that the higher the impedance of a load, the higher the maximum force of the tissue, but the lower the displacement. The peak energy stored in the cantilever probe resulting from a twitch is equal to half of the product of the peak twitch force and peak twitch displacement. For a linear relationship between force and displacement, the energy output as a function of displacement is a parabola with a global maximum in the middle (Fig. 6b). This energy maximum represents the maximum energy that a single twitch can transmit to a linear elastic load, such as the cantilever probe.

The performance of an engineered muscle construct and the impedance of the load it will drive should match for the muscle to transmit the most energy per contraction cycle to the load. This is clearly shown in Figure 6b. There is maximum energy transmission when the cantilever with an

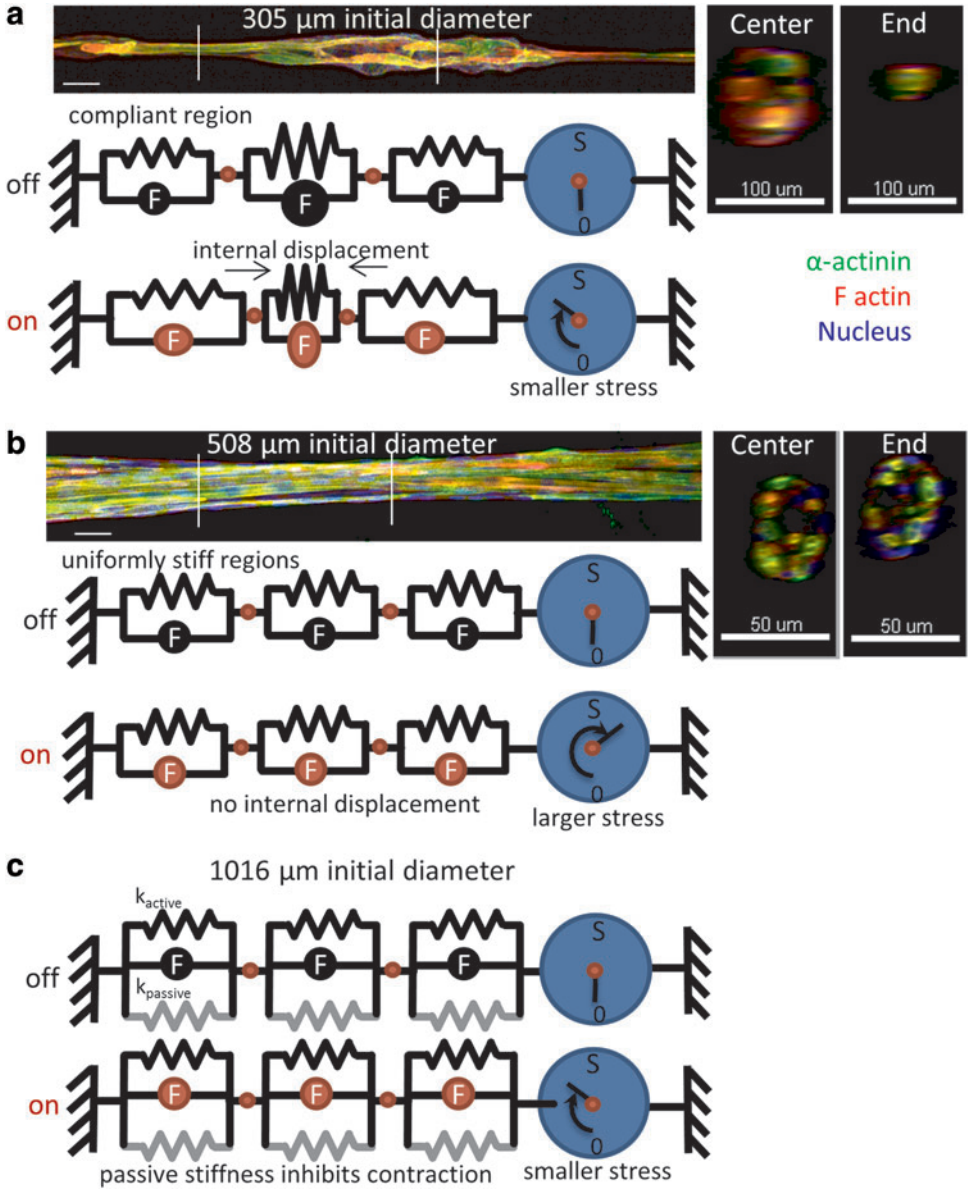

FIG. 5. Compliance model. Diagram of consequences of nonuniform strip development **(a)** versus uniform strip development **(b)** showing that compliant regions in the tissue result in internal displacements of the tissue that decrease the muscle's transmission of mechanical energy to an external load. **(c)** As the diameter increases, there is a greater volume of passive material that acts as stiffness to decrease contraction stress generation. Unspecified scale bars are 50 μm. Color images available online at www.liebertpub.com/tea

intermediate stiffness of 0.023 N/m is used. Notice that the energy transmitted to the stiffest cantilever results in the highest force, but not the highest energy transmission of the four probes used. Thus, the system presented here has been used to find impedance that maximized the output energy and that it is not equal to the impedance that produces the maximum output force.

Discussion

Using the mechanical characterization system described here, three key observations about engineered muscle constructs have been made. First, optical stimulation of myotubes formed from cells transfected with ChR2-encoding DNA is potentially as powerful as electrical stimulation if the muscle constructs are developed sufficiently. Second, there exists an optimal form factor at which to grow muscle tissue constructs seeded in a 3D scaffold where the performance metric is contraction performance per unit volume. Third, there exists an optimal load impedance to drive with an individual muscle construct where the performance metric is energy transmission to a load.

The key observation about optical stimulation broadens the potential use of optically stimulated muscle tissue. Muscle tissue that can be optically stimulated has been presented, but has not yet been methodically compared with electrical stimulation.[9] The proposed benefits of optical stimulation over electrical stimulation include having no need to use potentially invasive electrodes and the high spatial–temporal accuracy in stimulating specific muscle cells that may exist near other muscle cells. However, a significant question existed about the performance of optical stimulation. We show here that if the performance of the muscle tissue is average or above, optical and electrical stimuli produce similar twitches. This is likely due to superior strips having more highly developed contractile myotubes. This results in a greater proportion of functional myotubes that are not optically excitable. Another possibility that has not been shown explicitly

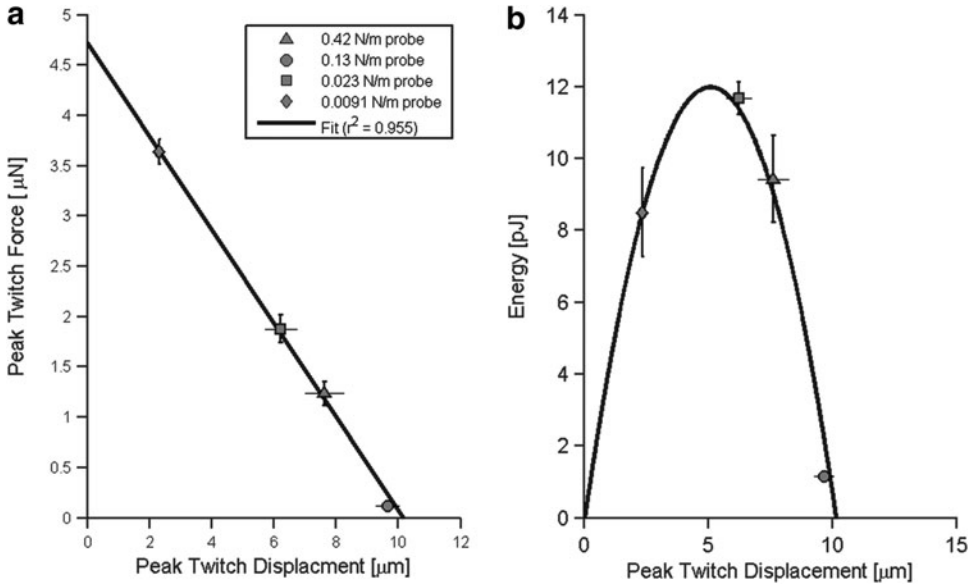

FIG. 6. Tissue performance under varying load conditions of a typical well-performing construct. **(a)** Peak twitch force and peak twitch displacement for a single tissue stimulated while laterally pulling the tissue with four different cantilevers of different stiffnesses. **(b)** Peak energy stored in the probe cantilever as a function of tissue displacement under four different cantilever loads. The straight line in **(a)** is a linear regression fit to the force–displacement data, while the parabola in **(b)** is the fit derived from the linear regression found in **(a)**. The maximum energy is produced in the middle of the force–displacement characteristics. Note: probe stiffness values are not equal to the geometry-corrected effective stiffness seen by the tissue. Error bars represent standard deviation. Error bars are smaller than the symbol where not shown.

is that immature/poor performing myotubes may need a greater level of stimulation than optical stimulation can provide. Further exploration of this phenomenon may provide valuable insights on how myotubes develop. With the results presented here, knowing that optical stimulation can produce similar results to electrical stimulation, future research may be conducted with optogenetic muscle tissue without the potential concern for vastly inferior performance.

The next key observation is about optimal form factor. There is an optimal strip diameter that produces the maximum twitch stress due to two conflicting requirements for the strip diameter. One is that the contractile cell density decreases as diameter increases, and the other is that the uniformity of the strip cross section decreases as the diameter decreases. These two phenomena can be put together in the simple linear component model shown in Figure 5 to predict the results in Figure 4.

Considering the first phenomenon, for larger diameter strips, diffusion-limiting processes discourage myotube formation within the central region of the construct, yielding fewer myotubes per cross-sectional area. This has been shown previously[17] where the volume of α-actinin is used as a surrogate of myotube volume. Additionally, if there are fewer cells near the central region to degrade the scaffold, then more scaffold will exist in the central region, resulting in increased passive scaffold the tissue must work against, as diagramed in Figure 5c. A simple model of this first phenomenon assumes that the cross section of the tissue has two regions: (1) an outer annulus of contractile tissue and (2) an inner disk of noncontractile scaffold. In the model, the thickness of the contractile ring/annulus is assumed to be $\sim 100\,\mu m$. When the thickness of the construct is this value or lower, all of the tissue is modeled as contractile. As the thickness of the construct becomes larger, a noncontractile region in the center begins to grow. Reported values of fibrin stiffness ($\sim 1\,kPa$) were used to model this inactive region.[18] The contractile region is modeled as producing $\sim 1\,kPa$ of peak stress based on observation and previous research,[6] and the stiffness of the cantilever load that the tissue is working against is modeled as $\sim 0.01\,N/m$, which is similar to the stiffness used to gather the data. This model of the effects of cell density results in the descending regions of the full model plotted in Figure 4c and d, where the final tissue diameter $> 150\,\mu m$.

The other phenomenon modeled is the greater degree of nonuniformity for smaller diameter constructs. This is modeled as compliant elements in series as shown in Figure 5 where exemplary strips are shown. Significant nonuniformities exist for smaller diameter strips because forces generated by individual myotube formation and development generate significant stress that causes necking of the hydrogel material lacking in differentiated myotubes. This does not happen in thicker constructs because the larger cross-sectional area of hydrogel is able to resist necking as individual myotubes mature over time. The overall stiffness is dominated by the most compliant elements. It has previously been reported that variation of the smallest strips (250 μm initial diameter) vary in diameter by 25%.[17] The effect of diameter nonuniformity on stiffness can be modeled as two springs in series having different stiffnesses. If the strip is simply modeled as two halves, with one having 75% of the mean diameter and the other having 125% of the mean diameter, then the effective stiffness of this structure is $\sim 65\%$ of a uniform structure having a constant diameter under the assumption that stiffness is proportional to the diameter squared. This disparity decreases to zero as the initial pin diameter increases. This model of nonuniformity

results in the decreasing performance as tissue diameter decreases. See the curves in Figure 4c and d where final tissue diameter $< 120\,\mu m$. While more detailed models are possible, this was the simplest model based on the physics of the system that captures the general trend observed in the twitch data. This same model fits well with both the stress and forces generated by the tissues.

Concerning the variation in twitch force between individual strips, there is greater variability in smaller construct twitch performance due, in large part, to the greater dependence on individual myotubes. Individual myotube performance varies from one cell to the next. The performance of the smaller diameter constructs varies more significantly than the larger constructs, because larger constructs have a greater number of myotubes to average performance over as can be seen in Figure 5a and b.

The best performing strip diameter was $500\,\mu m$ and generated an average twitch stress of 1.28 kPa. This is in line with high-performance muscle constructs reported in the literature.[19–21] Using an optimal initial diameter of $500\,\mu m$, tissues outperformed tissues using $250\,\mu m$ by more than 60% and tissues using $760\,\mu m$ by 105%. It is important to note that some articles report maximum twitch stress generation using a modified area in their calculation. Hinds *et al.* report a specific twitch force (stress generation) after they normalize by the average cross-sectional area of the active muscle layer. Lam *et al.* report their specific twitch force using an effective diameter, that is, the diameter of the constructs minus the area of the gel. The fact that research groups subtract the inactive central region of the tissue is in line with our findings of performance drop for larger diameter strips. It is important to also bear in mind that isometric force measurements, which are those typically reported, will be larger than forces measured against a compliant load.

The existence of an optimal form factor implies that a full-size skeletal muscle should be constructed as a bundle of the fascicle-like strips, each having the optimal diameter rather than one monolithic bulk. As *in vivo* muscles have a hierarchical structure, *in vitro*-grown skeletal muscles too should be constructed as a collection of optimal fascicle-like strips. When comparing twitch performance to other constructs made from bulk hydrogels, the directly measured generated stress is roughly twice as much. This is even more impressive given that the maximum stress measured in the system is not with isometric contractions, but with contractions against a compliant load, and that an immortalized cell line is used here rather than primary derived myocytes typically used in bulk hydrogel constructs, which tend to have superior contraction performance to cell lines.

The final key observation is about characterizing a tissue to find optimal impedance for energy transmission. By using the optimally stiff cantilever, 12 pJ of energy per twitch was transferred to the load. This demonstrates the utility of this unique tissue characterization platform. Furthermore, more complex characterization of muscle tissue performance using this system is possible. This system may be used to characterize muscle tissue working against a wide variety of impedance loads from linear stiffness (as presented here) to nonlinear time-dependent loads relevant to tissue engineering. In its current state, the system cannot measure initial tension or isometric tension because a measurable displacement is required to make a measurable force measurement; however, further advancement to the system to make these measurements and others is the subject of future work.

The cantilever probe loads presented are all simply linear elastic impedances, but do not need to be. Loads with dynamic impedance such as inertia and damping may also be implemented. Loads may include hydrodynamic conditions and/or highly nonlinear materials. The probe loading conditions may be made to match the loading conditions the tissue will be under when eventually put into use. Additionally, thanks to the similar performance to electrical stimulation, optical stimulation may be used to quickly and easily test any individual tissue under these arbitrary loading conditions. A valuable potential use will be testing constructs using cardiomyocytes instead of skeletal muscle cells. Cardiac muscle operates exclusively in a twitch-like manner and drives a hydrodynamic load as it pumps. Using this system, heart muscle tissue may be more fully characterized than isometric characterization can do alone.

The key findings of engineered muscle tissue as well as the characterization system presented here will be used to advance the field of muscle tissue research, muscle-related drug testing, and scaling engineered muscle constructs to produce muscle tissue systems of much larger size.

Acknowledgments

This material is based on work supported, in part, by the National Science Foundation under Grant No. CBET-0939511, the Science and Technology Center for Emergent Behaviors of Integrated Cellular Systems (EBICS), and, in part, by the Singapore-MIT Alliance of Research and Technology, BioSyM IRG.

Disclosure Statement

No competing financial interests exist.

References

1. Rhim, C., Lowell, D., Reedy, M., Slentz, D., Zhang, S., and Kraus, W., *et al.* Morphology and ultrastructure of differentiating three-dimensional mammalian skeletal muscle in a collagen gel. Muscle Nerve **36,** 71, 2007.
2. VanDusen, K.W., Syverud, B., Williams, M., Lee, J., and Larkin, L. Engineered skeletal muscle units for repair of volumetric muscle loss in the tibialis anterior muscle of a rat. Tissue Eng Part A **20,** 2920, 2014.
3. Wang, K., McCarter, R., Wright, J., Beverly, J., and Ramirez-Mitchell, R. Viscoelasticity of the sarcomere matrix of skeletal muscles. The titin-myosin composite filament is a dual-stage molecular spring. Biophys J **64,** 1161, 1993.
4. Brooks, S.V., and Faulkner, J.A. Forces and powers of slow and fast skeletal muscles in mice during repeated contractions. J Physiol **436,** 701, 1991.
5. Gordon, A.M., Huxley, A.F., and Julian, F.J. The variation in isometric tension with sarcomere length in vertebrate muscle fibres. J Physiol **184,** 170, 1966.
6. Dennis, R.G., and Kosnik, P.E. Excitability and isometric contractile properties of mammalian skeletal muscle constructs engineered in vitro. In Vitro Cell Dev Biol **36,** 327, 2000.

7. Chan, V., Asasda, H.H., and Bashir, R. Utilization and control of bioactuators across multiple length scales. Lab Chip **14,** 653, 2014.
8. Vandenburgh, H., Shansky, J., Benesch-Lee, F., Barbata, V., Reid, J., and Thorrez, L., *et al.* Drug-screening platform based on the contractility of tissue-engineered muscle. Muscle Nerve **37,** 438, 2008.
9. Sakar, M.S., Neal, D., Boudou, T., Borochin, M.A., Li, Y., Weiss, R., Kamm, R.D., Chen, C.S., and Asada, H.H. Formation and optogenetic control of engineered 3D skeletal muscle bioactuators. Lab Chip **12,** 4976, 2012.
10. Boudou, T., Legant, W.R., Mu, A., Borochin, M.A., Thavandiran, N., Radisic, M., *et al.* A microfabricated platform to measure and manipulate the mechanics of engineered cardiac microtissues. Tissue Eng Part A **18,** 910, 2012.
11. Johnston, I., McCluskey, D., Tan, C., and Tracey, M. Mechanical characterization of bulk Sylgard 184 for microfluidics and microengineering. J Micromech Microeng **24,** 035017, 2014.
12. Lötters, J.C., Olthuis, W., Veltink, P.H., and Bergveld, P. The mechanical properties of the rubber elastic polymer polydimethylsiloxane for sensor applications. J Micromech Microeng **7,** 145, 1997.
13. Vandenburgh, H.H., Swasdison, S., and Karlisch, P. Coputer-aided mechanogenesis of skeletal muscle organs from single cells *in vitro*. FASEB J **13,** 2860, 1991.
14. Nagamine, K., Kawashima, T., Sekine, S., Ido, Y., Kanzaki, M., and Nishizawa, M. Spatiotemporally controlled contraction of micropatterned skeletal muscle cells on a hydrogel sheet. Lab Chip **11,** 513, 2011.
15. Kim, T., McCall, J.G., Jung, Y.H., Huang, X., Siuda, E.R., *et al.* Injectable, cellular-scale optoelectronics with applications for wireless optogenetics. Science **340,** 211, 2013.
16. Dennerll, T.J., Joshi, H.C., Steel, V.L., Buxbaum, R.E., and Heidemann, S.R. Tension and compression in the cytoskeleton of PC-12 neurites II: quantitative measurements. J Cell Biol **107,** 665, 1988.
17. Neal, D., Sakar, M.S., Ong, L.L.S., and Asada, H.H. Formation of elongated fascicle-inspired 3D tissues consisting of high-density, aligned cells using sacrificial outer molding. Lab Chip **14,** 1907, 2014.
18. Duong, H., Wu, B., and Tawil, B. Modulation of 3D fibrin matrix stiffness by intrinsic fibrinogen-thrombin compositions and by extrinsic cellular activity. Tissue Eng Part A **15,** 7, 2009.
19. Huang, Y.C., Dennis, R.G., Larkin, L., and Baar, K. Rapid formation of functional muscle *in vitro* using fibrin gels. J Appl Physiol **98,** 706, 2005.
20. Lam, M.T., Huang, Y.C., Birla, R.K., and Takayama, S. Microfeature guided skeletal muscle tissue engineering for highly organized 3-dimensional free-standing constructs. Biomaterials **30,** 1150, 2009.
21. Hinds, S., Bian, W., Dennis, R.G., and Bursac, N. The role of extracellular matrix composition in structure and function of bioengineered skeletal muscle. Biomaterials **32,** 14, 2011.

Address correspondence to:
Haruhiko Harry Asada, PhD
Department of Mechanical Engineering
Massachusetts Institute of Technology
77 Massachusetts Avenue
Room 1-007
Cambridge, MA 02139

E-mail: asada@mit.edu

Received: May 30, 2014
Accepted: February 23, 2015
Online Publication Date: April 29, 2015